Materials Research Proceedings 28 (2023) 1765-1774 https://doi.org/10.21741/9781644902479-191

Coefficient of friction of cemented carbides machined by sinking EDM

PETERSEN Timm[1,a,*], KÜPPER Ugur[1,2,b], HERRIG Tim[1,c] and BERGS Thomas[1,2,d]

[1]Laboratory for Machine Tools and Production Engineering (WZL) of RWTH Aachen University, Campus Boulevard 30, 52074 Aachen, Germany

[2]Fraunhofer Institute for Production Technology IPT, Steinbachstr. 17, 52074 Aachen Germany

[a]t.petersen@wzl.rwth-aachen.de, [b]u.kuepper@wzl.rwth-aachen.de, [c]t.herrig@wzl.rwth-aachen.de, [d]t.bergs@wzl.rwth-aachen.de

Keywords: Sinking Electrical Discharge Machining, Cemented Carbide, Coefficient of Friction

Abstract. Cemented carbides possess properties that predestine them as a durable tool. However, these properties hinder conventional machining, which is why Electrical Discharge Machining (EDM) is a promising alternative. Three different EDMed cemented carbides were compared with a ground surface in a pin-on-disk test setup. They were evaluated under dry and lubricated conditions with two distinct antibody materials. The tests did not reveal a correlation between the surface roughness of the cemented carbide pins and the coefficient of friction. However, some test sets yielded very different results, which is why particular considerations should be made with new sliding compositions.

Introduction

The requirements for tools used in forming processes are subject to a continuous increase [1]. On the one hand, higher strength materials are used as workpiece material in forming in order to implement lightweight design. On the other hand, the tolerances become narrower to allow net-shape production, reducing subsequent machining steps and increasing material efficiency. Both developments result in higher tool loads and thus shorter tool life time [2,3]. Therefore, it is part of current research to investigate the properties and applicability of new tool materials such as cemented carbides [4,5]. Cemented carbides can resist high compressive stresses and are significantly harder than conventional tool materials. This makes cemented carbides substantially more resistant to wear [6]. However, these properties hinder conventional machining simultaneously. Grinding is only possible in the case of certain geometries and milling proves to be very challenging [7]. One alternative applied to machine forming tools from cemented carbides is electrical discharge machining (EDM) [8]. Due to its thermal working principle, EDM is able to machine workpieces independently from their mechanical properties [9]. EDM employs several thousand discharges per second, which are temporally and spatially very confined. These discharges consist of plasma, which melts and evaporates the adjacent material. On the one hand, not all material that is molten is also removed from the discharge location and thus leads to the formation of a recast layer, also known as white layer due to its appearance in cross sections. On the other hand, not all heat that is transferred from the plasma to the workpiece is involved in melting or evaporating the material. Some of the heat is transported further below the surface but only heats the material up to a certain temperature. In some cases it can reach the corresponding phase transformation temperature. Because the amount of heat is very little for each single discharge, it is quickly dissipated into the periphery. This leads to rapid cooling and in some cases a freeze of the material in the current phase and geometry [10]. The tensions resulting from this process can lead to residual stresses and cracks. Especially cemented carbides are prone to these effects, because they consist of two or more different phases with different thermophysical

properties. One way to reduce the impact on the workpiece is the application of a sequence of different machining steps each subsequent one with lower heat input. This sequence allows for productive machining whilst keeping the effect on the rim zone as small as possible. For cemented carbides, it has been proposed [11] to use needle type discharges in order to optimise production with both objectives in mind. It has been shown that this approach can be applied successfully for fine and ultra-fine grained cobalt cemented tungsten carbides [12]. It could also be seen that the surface roughness changed from one machining step to the other. Therefore, the objective of this research is to identify the influence three different surface topographies of two different cemented carbide grades have on the sliding behavior with two different antibodies and tested in two different lubrication conditions. Several authors have published research regarding the tribological behaviour of cemented carbides [13,14], because of their properties that destine them for the use as forming tools. Another aspect that is regularly researched is the tribological performance of surfaces produced by EDM. It has been shown, that the craters can serve as reservoirs for the lubricant or to reduce particles in the contact zone [15,16]. Additionally, Sari et al. [17] compared the load carrying capacity of wire EDMed gears to those manufactured with profile grinding and found that the characteristic surface structure resulting from the EDM process leads to beneficial tribological conditions in rolling contact. They attributed this to the statistical and non-directional crater structure resulting from EDM, which allows the roughness to get flattened instead of resisting the load and thus reducing the peak stresses in the material. However, it must be expected that the effects are different in this case because the investigated material was hardened 16MnCr5 instead of the present cemented carbide, which will most likely not be reshaped by the counterbody. In contrast, Bergs et al. [18] did not get the same results in a disk-on-disk test comparing wire electrical discharge turning (WEDT) to grinding. In their case, the flattening of the WEDTed surfaced did not yield the same surface roughness as the ground specimen. However, it has to be noted that the WEDT processes is more challenging than WEDM because of an increased punctiform heat input and the need for a precise runout in combination with the moving wire. The present paper aims to combine both elements and investigate the tribological behavior of cemented carbides machined by EDM.

Experimental Setup

The experimental setup was chosen according to previous investigations, however, some alterations have been made. The process of specimen preparation was the same as previously [19]. The only difference lies in the geometry of the tested pin. For the present investigations, the specimens had a convex contact area and the body of the pin was 10 mm by 10 mm. The radius of the convex area was 20 mm. As depicted in Fig. 1 on the left, the cemented carbide pins were cut from blocks via wire electrical discharge machining (WEDM) with an oversize on the top of the pin of 1 mm. This oversize was then removed via sinking electrical discharge machining (SEDM). The oversize and the machining technology of SEDM were chosen in order to make the material experience the roughing steps of the technology whilst still reaching the best available surface finish of Ra = 0.2 µm. The technology was applied three times in a different way. The first pins were created whilst only applying the first machining step. This machining step is called roughing. The second set of pins was created using the first machining step and all steps necessary to reach a surface roughness of Ra = 1 µm. This machining operation is called finishing. The third set of pins was created using all the previous machining steps and all additional machining steps in order to reach a surface roughness of Ra = 0.2 µm. This machining operation is called super-finishing. Both GFMS EDM machines used hydrocarbon oils as dielectric. While the Cut 2000 X Oil Tech used IonoFil 100, the Form 2000 VHP used Ionoplus IME-MH, both by the company oelheld. The tool materials were 0.2 mm brass wire for WEDM and copper tungsten (WCu) with 80 wt% for SEDM. The materials of the pins were CTF30 and UMG01 by Ceratizit [20]. CTF30 consists of 15 wt% cobalt and tungsten carbide grains with a size of 0.8 - 1.3 µm, whereas UMG01 does not

contain a significant amount of binder material and consists of tungsten carbide grains with a size of 0.2 µm. The friction test was conducted according to previous investigations [19, 21]. The setup can be seen in Fig. 1 on the right hand side. The cylindrical antibody was mounted on a lathe and rotated with a constant angular velocity of $\omega = 312.5\ min^{-1}$ resulting in a surface velocity relative to the pin of $v = 6.25\ m \cdot min^{-1}$. Two different antibody materials were used in this investigation: 42CrMo4 and 16MnCr5. The radii of the cylinders were r = 20 mm each. The pins were pressed on the rotating cylinder with a force of $F_n = 5000$ N. The force F_n was controlled with a 9011A force sensor and the resulting force F_t with a 9257B dynamometer, both by Kistler. In order to evaluate the effect the eroded surface has on the transport of lubricant, the tests were conducted with and without minimal quantity lubrication. In the case of lubrication, the Lubrimat L60 by Steidle was used to apply single drops of lubricant every few seconds.

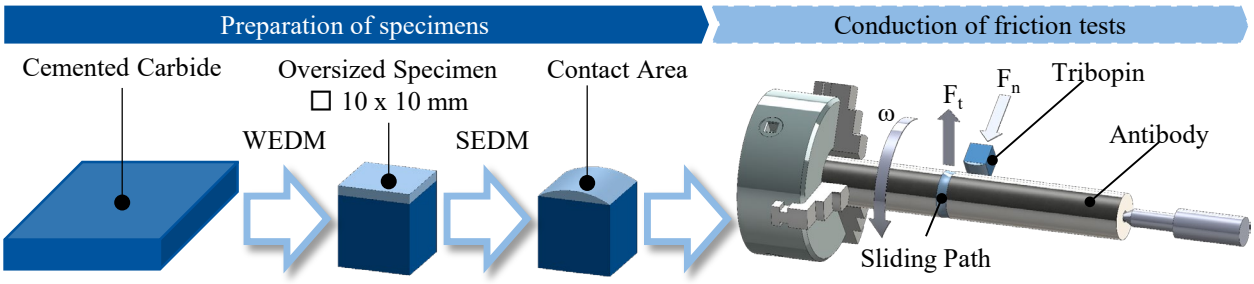

Fig. 1. Process of preparation of specimen and test setup according to [21].

Three different outputs from the tests were evaluated. Firstly, the tangential force F_t resulting from the applied force F_n and the rotation ω were measured. An arrow indicating this force F_t can be seen in Fig. 1 on the right. However, because of the difficulties described in a previous publication [19], where the investigations were conducted according to the setup schematically depicted in Fig. 2, top left was changed. There, the theoretical contact between the specimen and the antibody was a line. Because material was quickly sticking to the surface of the specimen and the antibody was reshaped during the test procedure, the stick-slip effect occurred. This caused strong vibrations and increased the overall level of the detected tangential force, which can be seen in Fig. 2, left bottom. In order to prevent the stick-slip effect and the resulting vibration, the test setup was revised according to the schematic drawing in Fig. 2, right top. Here two cylinders can be seen that are placed orthogonally to each other. The actual pins were only a cuboid cutout of the rear cylinder, which does not affect the contact area. Both cylindrical surfaces have the same radii of r = 20 mm. This setup theoretically causes a point contact, which reduces the risk of vibration. It can be seen in the graphs comparing the two setups that the revised setup is able to measure the force without vibrations or deviations. The subsequent evaluation of the measurements is a lot more stable and reliable since the section to be evaluated does not have to be chosen manually.

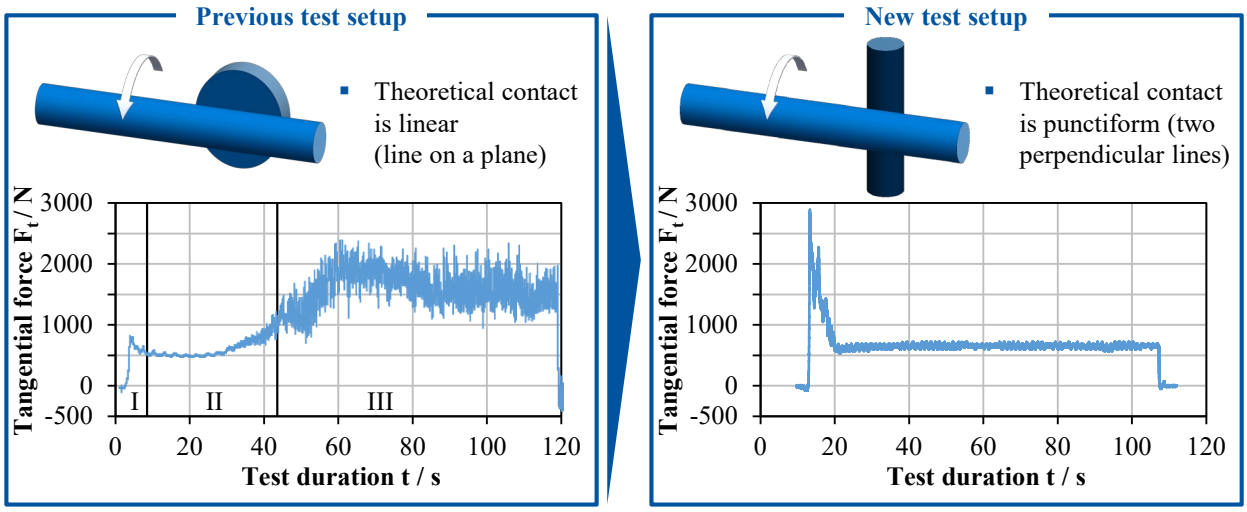

Fig. 2. Comparison of previous and revised test setup [19].

The second and third output from the investigation are the surfaces of the specimen and the antibody. Both were investigated using the optical microscope Smartzoom 5 by Zeiss. For comparison, some cemented carbide pins were ground to the desired shape with a diamond grinding wheel bound with artificial resin. Since each experiment was conducted thrice, the according number of pins had to be created from the corresponding materials. This totaled in a number of 96 pins, 48 from each cemented carbide grade and 12 of each surface finish.

Results

In order to give an idea of the surfaces that were created with the different machining operations described in the experimental setup, Fig. 3, left depicts the average surface roughnesses of all pins used in this investigation. For statistical reasons, all pins were tactilely measured three times with a Waveline 800 by Jenoptik. The colours of the columns indicate the material, with dark blue being CTF30 and light blue being UMG01. As expected, it can be seen that the surface roughness decreases with the increased number of machining steps. However, a clear difference between the two materials can be perceived as well. The surface roughness of UMG01, the small grained and binderfree material is significantly smaller for all compared surface conditions. As described by Bergs et al. [22], this difference cannot entirely be attributed to the smaller grain size. For the roughed specimen, the white layer, which consists of molten and resolidified material, is significantly larger than the largest protruding WC grains.

On the right hand side of Fig. 3 the average coefficient of friction is depicted. The coefficient of friction μ is the quotient of the two forces F_t and F_n as shown in Eq. 1. Because the applied force F_n varied slightly from test to test, both forces were measured and averaged over the same duration as denoted in Fig. 2, right bottom.

$$\mu = \frac{F_t}{F_n} \tag{1}$$

In this part of the investigation, the averages are calculated over all surface conditions of the pins. The purpose of this diagram is to highlight the difference between the two antibody materials. However, the differences are marginal. For both antibody materials, the average coefficient of friction (COF) appears to be the same with respect to the lubrication condition. It can be noted that the coefficients of friction (COFs) with dry 42CrMo4 are slightly larger than those with 16MnCr5, while the deviation is a little larger as well. In the lubricated condition, this result is turned around and the COFs with 42CrMo4 are slightly smaller than those with 16MnCr5. From the present

results it can be presaged that the described effects are a little more dominant with CTF30 than with UMG01, while there is no difference detectable within the cemented carbide pins with 16MnCr5. Regarding this evaluation it can be stated that the antibody materials do not seem to have a strong effect on the COF.

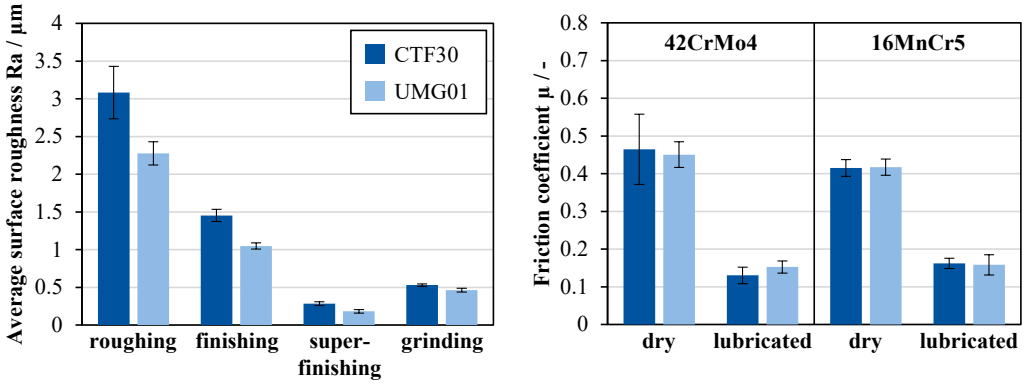

Fig. 3. Average surface roughness of the cemented carbide pins and the average coefficient of friction for both antibody materials and both lubrication conditions.

A more detailed analysis of the COFs is depicted in Fig. 4. Here both cemented carbides and all surface and lubrication conditions are separately displayed for the antibody material 42CrMo4. On the left hand side, the COF is shown as it appeared without any lubrication and on the right hand side it is shown as it appeared with the application of lubricant. Regarding the dry condition, a large deviation can be seen for the ground CTF30 specimens. Here one ground pin yielded a COF of 0.75, which was much higher than all the other results. In general, there is no correlation between the surface roughness and the COF. For CTF30, the worst COF of the eroded specimen resulted from the finished pins. The roughed and super-finished surface conditions resulted in the lowest COFs. For the eroded UMG01 pins, no significant difference between the COFs can be recognized and it should be noted that these results have very little deviations. Only the ground UMG01 pins have significantly lower COF of around 0.4.

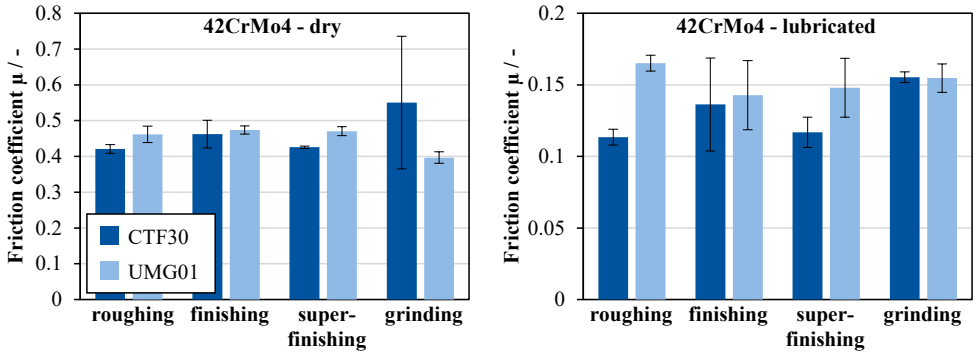

Fig. 4. Coefficients of friction for 42CrMo4, all surface conditions of the cemented carbide pins and for both lubrication conditions.

The deviations appearing in the diagram on the right hand side of Fig. 4 appear to be significantly larger than those from the unlubricated surface condition on the left hand side. However, it needs to be emphasized that the scale is different and the largest deviations on the right are slightly smaller than those of the finished CTF30 pins on the left, which is the largest

without considering the ground CTF30 pins. The lubricated CTF30 pins show a very similar appearance to the unlubricated ones. The finished CTF30 pins result in the largest COF for the eroded pins and the roughed and super-finished pins result in very similar COFs. All eroded CTF30 pins result in a lower COF than the ground pins. This might be caused by an effect suggested by Sari et al. [17]. They described the capability of the discharge craters to transport a lubricating medium into the contact area. They found that the durability of gears machined by EDM can be higher because of this effect and in contrast to the doubts created by the harmful effect EDM has on the surface integrity. However, the same effect cannot be seen for the pins made of UMG01, even though the ground pin has almost exactly the same COF as the one made from CTF30. The finished and super-finished UMG01 pins have a slightly lower average COF, but the deviations are large enough to range them on the same level as the ground pin. Furthermore, in contrast to CTF30, the roughed UMG01 pins have the highest overall COF for this lubrication condition and antibody material. Especially, when comparing the two results for the roughed pins, which both have a very little standard deviation, it becomes apparent that there must be a difference resulting from the material of the specimens.

The second antibody material investigated was 16MnCr5. The resulting COFs are displayed in Fig. 5, where the non-lubricated condition is shown on the left and the lubricated condition is shown on the right. For the dry condition, no successful tests could be conducted for the roughed and the ground UMG01 specimen. The specimen broke or the force was quickly overreaching the measurement scale, indicating an upcoming breakage. This happened for all the specimen of the corresponding test series even though the tests were conducted in a randomized order, which reduces the chances that this result is solely caused by an outlier. All other tests on this antibody material have worked in the same way as on 42CrMo4 and have shown the same force pattern as seen in Fig. 2. The remaining COFs from the dry constellation show very little variance. Neither the material of the specimen nor the applied surface finish seems to have a significant influence. In comparison to the antibody material 42CrMo4, which has an average COF for the dry condition of 0.46, the average COF is slightly lower with a value of 0.42. The lubricated condition displays a very different result. Here, the COFs vary throughout both investigated parameters. For CTF30, the differences are only slight, but it can been seen that the COF shrinks with a decreased surface roughness for the eroded specimens. The ground specimens however, yielded the highest COF, albeit not having the highest surface roughness. All results for CTF30 are within a smaller range than the results of UMG01. Especially, between the roughed and the finished specimens there is a large difference, with the prior having the smallest COF on this antibody material and the latter having the highest COF for all tests conducted under the lubricated condition. The super-finished and the ground UMG01 specimens have a very similar average COF, however, the deviation was larger for the super-finished specimens. When comparing the two antibody materials for the lubricated condition, it becomes apparent that 42CrMo4 yielded a lower average of 0.14 but the deviations in the test were significantly larger. In contrast, the average COF for the lubricated 16MnCr5 was 0.16 with a relatively small deviation. Additionally, the comparison of the cemented carbide pins for the lubricated tests also reveals an interesting difference. For 42CrMo4, UMG01 does not appear to be affected by its surface condition. In contrast, for 16MnCr5, UMG01 yielded different results for different surface conditions. The results for CTF30 can be read vice versa.

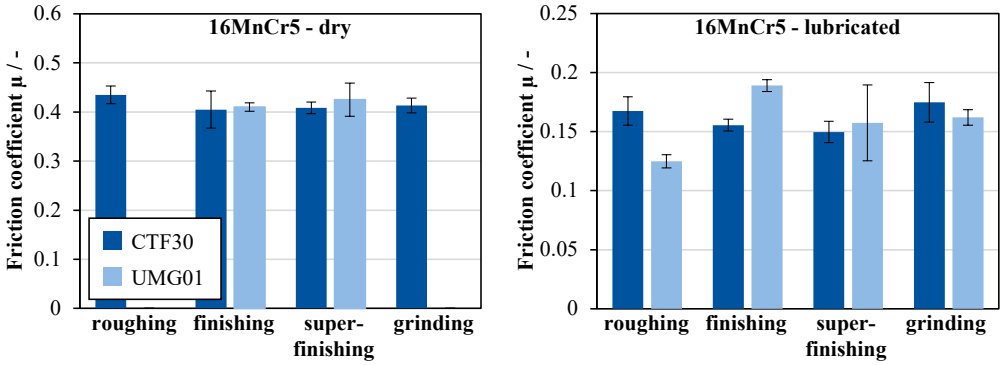

Fig. 5. Coefficients of friction for 16MnCr5, all surface conditions of the cemented carbide pins and for both lubrication conditions.

The results for the COF contrast the results presented by Llanes et al. [23], who found that the COF correlates with the surface roughness. However, they used a scratch test setup, where the indenter was a spherical tip diamond with a radius of 50 µm and the antibody was the EDMed cemented carbide. In general, the results are in good agreement with literature regarding tests conducted in dry conditions [14,24] and are only slightly higher in the lubricated condition than the laser textured specimen tested by Fang et al. [13].

In Fig. 6 and Fig. 7, the surfaces of the cemented carbide pins can be seen after the tests. In Fig. 6, the pins tested with 42CrMo4 as antibody material are depicted and in Fig. 7 the pins tested with 16MnCr5 are shown. In both figures, several broken pins are displayed. However, most of them broke when the test setup was disassembled. In Fig. 6, only the super-finished UMG01 pin number 3 broke during the test. For Fig. 7, all the super-finished and the first roughed UMG01

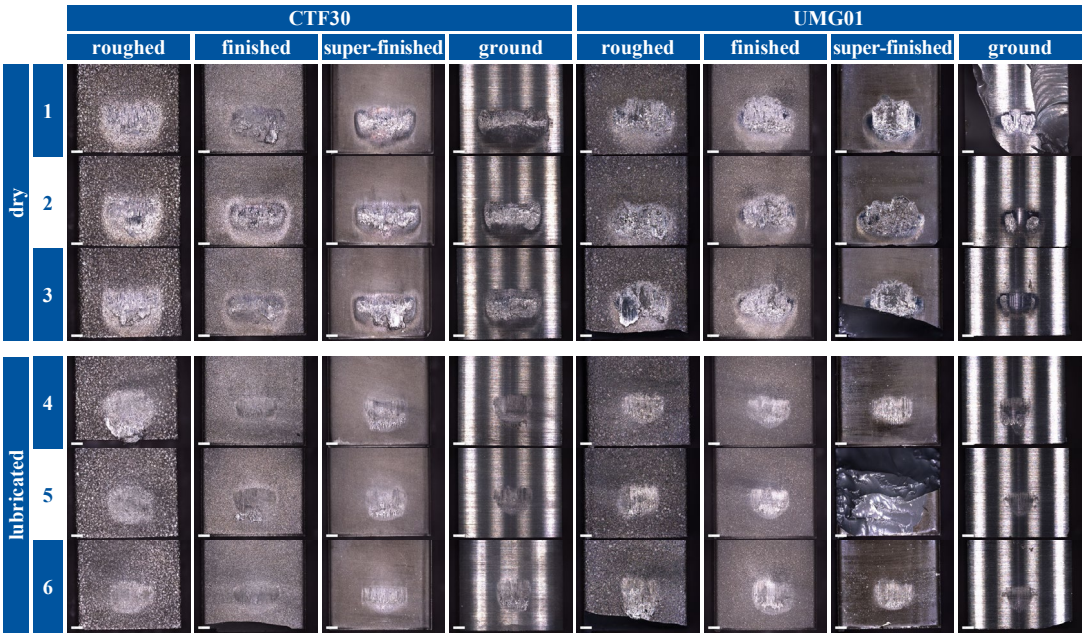

Fig. 6. Microscopic images of the surfaces of all pins tested on 42CrMo4.

pins broke in the test without lubrication. The remaining two roughed UMG01 pins were causing an overload in the measurement system and were therefore stopped. All the pins that broke first caused an overload, which is why these pins were accounted for as broken.

For both antibody materials, different regions are present on most cemented carbide pins. On the one hand, there are regions which appear to be flattened and on the other hand there are regions that have accumulated material. Even though the tested cemented carbides are significantly harder than the tested shafts, profilometry revealed that the tips of the profile have been flattened. An energy dispersive X-ray spectroscopy (EDX) has been conducted to reveal that all the material that appears to be bulged has in fact migrated from the test shafts and is not rearranged material from the cemented carbide pin.

When comparing the microscopic images from Fig. 6 and Fig. 7, a difference in the size of the imprint can be observed. For the antibody material 42CrMo4, the imprint appears significantly smaller than for the antibody material 16MnCr5. Similarly, the imprints on the shafts are larger on 16MnCr5 than on 42CrMo4.

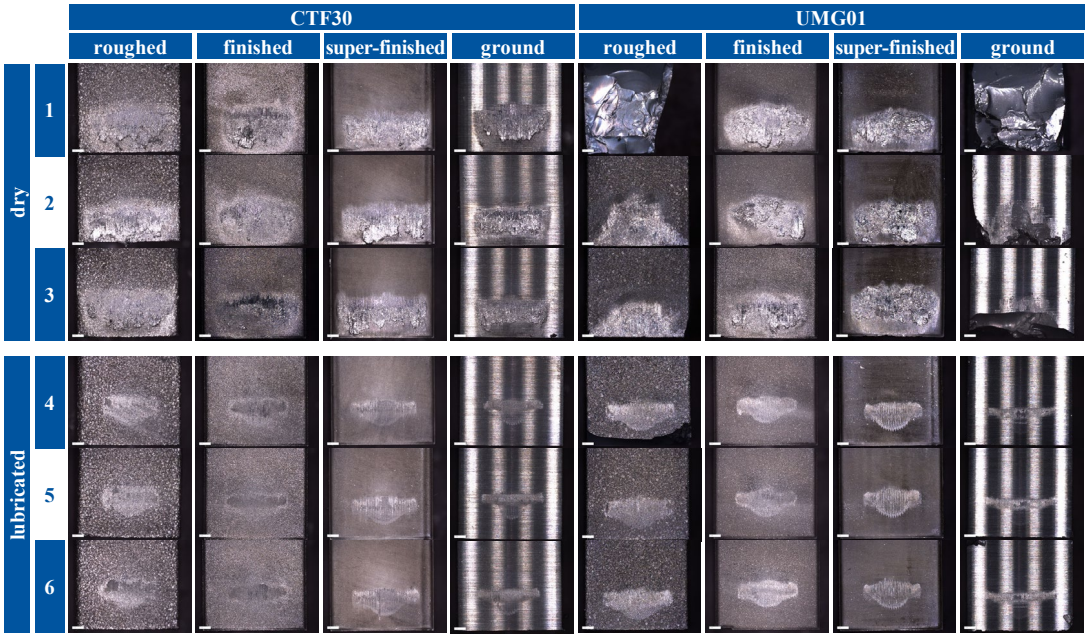

Fig. 7. Microscopic images of the surfaces of all pins tested on 16MnCr5.

Summary

The coefficient of friction of two distinct cemented carbides in contact with two different antibody materials was investigated in a dry and a lubricated setup. The cemented carbide pins were machined through sinking EDM to three different surface finishes and one set of pins was manufactured by grinding as a reference. Even though the surface roughnesses differed from one machining strategy to the other, no general correlations between the surface roughness and the COF could be found. Likewise, both antibody materials yielded similar results in the respective tests. Some test configurations, however, did show significant differences, which indicate the necessity to evaluate each configuration of materials and surface properties independently. This is especially obvious with the broken specimens from the series 16MnCr5, dry, roughed and ground. The friction reducing effect of the craters presumably present in the lubricated setup could not be identified with the same extend as it is in literature, which is attributed to the smaller dimensions of the craters found on cemented carbide surfaces.

Funding

The authors thank the German Research Foundation (DFG) for funding the DFG project BE 2542/42-2: “Analysis of discharge-dependent surface integrity of cemented carbide forming

dies machined by sinking EDM and its influence on the tribological characteristics and the resulting fatigue behaviour"(project number 290130034).

References

[1] F. Klocke, Manufacturing processes: Forming, Springer, Berlin, New York (2013) ISBN: 978-3-642-36772-4.
[2] U. Engel, J. Groenback, C. Hinsel, Tooling solutions for challenges in cold forging, Umformtechnik (2011).
[3] J. Cao, E. Brinksmeier, M. Fu, R.X. Gao, B. Liang, M. Merklein, M. Schmidt, J. Yanagimoto, Manufacturing of advanced smart tooling for metal forming, CIRP Annals, 68 (2019) 605-628. https://doi.org/10.1016/j.cirp.2019.05.001
[4] H. Voigts, R. Hild, A. Feuerhack, T. Bergs, Investigation of Failure Mechanisms of Cemented Carbide Fine Blanking Punches by Means of Process Forces and Acoustic Emission, in Forming the Future, Springer, Cham (2021) 1173-1187. https://doi.org/10.1007/978-3-030-75381-8_98
[5] O. Baer, A. Feuerhack, H. Voigts, T. Bergs, Investigation of the Mechanical Punch Loads during Fine Blanking of High-Strength Steels with Cemented Carbide, Procedia Manuf. 34 (2019) 90-100. https://doi.org/10.1016/j.promfg.2019.06.125
[6] L. Prakash, Editor, Comprehensive Hard Materials: Fundamentals and General Applications of Hardmetals, Elsevier, 2014. ISBN: 9780080965284.
[7] E.L. Silva, S. Pratas, M.A. Neto, C.M. Fernandes, D. Figueiredo, R.F. Silva, Multilayer Diamond Coatings Applied to Micro-End-Milling of Cemented Carbide, Materials 14 (2021) 3333. https://doi.org/10.3390/ma14123333
[8] K. Andreas, M. Merklein, U. Engel, Influence of Combined Hard and Fine Machining on the Surface Properties of Cemented Carbides, Tribology in Industry 34 (2012) 119-127.
[9] F. Klocke, W. König, Fertigungsverfahren: Abtragen, Generieren und Lasermaterialbearbeitung, Springer, Berlin, New York, 2007. ISBN: 9783540236504.
[10] R. Hess, P. Grethe, L. Heidemanns, T. Herrig, A. Klink, T. Bergs, Simulation based derivation of changed rim zone properties caused by thermal loadings during EDM process, Procedia CIRP 113 (2022) 41-46. https://doi.org/10.1016/j.procir.2022.09.117
[11] H. Juhr, H.-P. Schulze, G. Wollenberg, K. Künanz, Improved cemented carbide properties after wire-EDM by pulse shaping, J. Mater. Process. Technol. 149 (2004) 178-183. https://doi.org/10.1016/j.jmatprotec.2004.02.037
[12] T. Petersen, U. Küpper, A. Klink, T. Herrig, T. Bergs, Discharge energy based optimisation of sinking EDM of cemented carbides, Procedia CIRP 108 (2022) 734-739. https://doi.org/10.1016/j.procir.2022.03.113
[13] S. Fang, S. Klein, C.-J. Hsu, L. Llanes, C. Gachot, D. Bähre, Fabrication and tribological performance of a laser-textured hardmetal guiding stone for honing processes, Int. J. Refract. Metal. Hard Mater. 84 (2019) 105034. https://doi.org/10.1016/j.ijrmhm.2019.105034
[14] W. Zhao, N. He, L. Li, Friction and Wear Properties of WC-Co Cemented Carbide Sliding against Ti6Al4V Alloy in Nitrogen Gas, Adv. Mater. Res. 188 (2011) 49-54. https://doi.org/10.4028/www.scientific.net/AMR.188.49
[15] K.W. Liew, C.K. Kok, M.N. Ervina Efzan, Effect of EDM dimple geometry on friction reduction under boundary and mixed lubrication, Tribol. Int. 101 (2016) 1-9. https://doi.org/10.1016/j.triboint.2016.03.029
[16] R. Zhou, J. Cao, Q.J. Wang, F. Meng, K. Zimowski, Z.C. Xia, Effect of EDT surface texturing on tribological behavior of aluminum sheet, J. Mater. Process. Technol. 211 (2011) 1643-1649. https://doi.org/10.1016/j.jmatprotec.2011.05.004
[17] D. Sari, D. Welling, C. Löpenhaus, F. Klocke, A. Klink, Adjusting Surface Integrity of Gears Using Wire EDM to Increase the Flank Load Carrying Capacity, Procedia CIRP 45 (2016) 295-298. https://doi.org/10.1016/j.procir.2016.02.355

[18] T. Bergs, U. Tombul, D. Mevissen, A. Klink, J. Brimmers, Load Capacity of Rolling Contacts Manufactured by Wire EDM Turning, Procedia CIRP 87 (2020) 474-479. https://doi.org/10.1016/j.procir.2020.02.111
[19] T. Petersen, U. Küpper, T. Herrig, A. Klink, T. Bergs, Fracture Toughness and Tribological Properties of Cemented Carbides Machined by Sinking Electrical Discharge Machining, ESAFORM 2021 (2021) 13. https://doi.org/10.25518/esaform21.1518
[20] CERATIZIT, Complete programme wear parts 2015. https://www.ceratizit.com/uploads/tx_extproduct/files/GD_KT_PRO-0272-0915_SEN_ABS_V1.pdf. Accessed 19 June 2020.
[21] P.-M. Mattfeld, Tribologie der zinkphosphatfreien Kaltmassivumformung, Dissertation, RWTH Aachen University, Aachen, 2014. ISBN: 978-3-86359-195-3.
[22] T. Bergs, T. Petersen, U. Tombul, A. Klink, Analysis of the Influence of Surface Integrity of Cemented Carbides Machined by Sinking EDM on Flexural Fatigue, Procedia CIRP 87 (2020) 456-461. https://doi.org/10.1016/j.procir.2020.02.096
[23] L. Llanes, Influence of electrical discharge machining on the sliding contact response of cemented carbides, Int. J. Refract. Metal. Hard Mater. 19 (2001) 35-40. https://doi.org/10.1016/S0263-4368(00)00045-7
[24] K. Bonny, P. de Baets, W. Ost, J. Vleugels, S. Huang, B. Lauwers, W. Liu, Influence of electrical discharge machining on the reciprocating sliding wear response of WC-Co cemented carbides, Wear 266 (2009) 84-95. https://doi.org/10.1016/j.wear.2008.05.009